NJC

ROYAL SOCIETY OF CHEMISTRY

PAPER

View Article Online
View Journal | View Issue

Cite this: *New J. Chem.*, 2021, **45**, 8155

One-step construction of a novel AIE probe based on diaminomaleonitrile and its application in double-detection of hypochlorites and formaldehyde gas†

Xiaoye Wen,‡ Li Yan‡ and Zhefeng Fan *

Received 24th February 2021,
Accepted 7th April 2021

DOI: 10.1039/d1nj00932j

rsc.li/njc

As the environmental residues of formaldehyde and hypochlorites are very harmful to human health, a new simple and efficient aggregation-induced emission probe based on diaminomaleonitrile was designed and applied in the independent detection of hypochlorites and formaldehyde. The probe shows high selectivity and anti-interference ability against other potential competitive substances. ClO^- promotes the oxidized splitting of C=N in the probe, and induces evident color changes visible to the naked eye together with quenched fluorescence. The detection of ClO^- by this probe was fast, sensitive, and visible to the naked eye. The detection limit of the probe to ClO^- in the range of 0.70–20 μM is 18 nM. Through the condensation mechanism and with amine as the binding site of formaldehyde, the exposed amino group in the probe structure responds sensitively and efficiently to formaldehyde. The probe can effectively monitor 0.50–25 μM formaldehyde in aqueous solutions, with a detection limit as low as 42 nM. A portable solid sensor – a formaldehyde detection plate was built by directly covering the probe on a thin-layer chromatography plate. Thereby, formaldehyde gas can be effectively and sensitively detected, which offers a clue for developing solid-state formaldehyde-detection plates. The high experimental recovery rates prove that this new probe is highly promising in hypochlorite detection in the real water environment.

1. Introduction

Fluorescent probes have gradually been used as powerful tools to track small molecules in the environment and life systems, owing to their avoidance of sample pretreatment, low operational complexity, ease of visualization, fast response, high selectivity, and high sensitivity.[1–4] However, the existing fluorescent probes are monofunctional and only have single binding site targeting a specific analytical substance, and thus are severely restricted in practical applications. Research on multifunctional fluorescent probes with higher detection efficiency and lower costs is critical in developing and constructing fluorescence detection systems and is of very high significance and values.[5–7] Double- or multi-analyte responsive fluorescent probes have been designed to build probes with multiple reaction sites and to identify different substances through the analysis of different reaction mechanisms. Double-analyte fluorescent probes can be mainly divided into AND logics and OR logics.[8–10] The AND logic fluorescent probes can detect signals through the simultaneous or sequential action of more than one analyte.[11,12] On the contrary, the analytes in OR multi-site fluorescent probes can independently bind with the reaction sites and are mutually non-interfering, and thus possess higher accuracy and sensitivity.[13–15] In all, fluorescent probes with multiple detection sites are prospective methods for simultaneous detection of multiple chemical substances.

Hypochlorites are used in various fields, such as bleachers (paper plants), disinfectants (tap water, swimming pools) and cleaners.[16–18] The inhalation of trace hypochlorites can injure airway mucosas, leading to cough, asthma or even dyspnea, and the intake of high-dose hypochlorites can result in severe acute symptoms, such as pneumonedema.[19,20] Hence, prevention of accidental leakage of hypochlorites and establishment of fast and sensitive hypochlorite detection methods is extremely important. So far, fluorescent probes have been prepared and used in ClO^- detection, but their mechanisms are mostly based on the oxidizing reaction of ClO^- with different functional groups (*e.g.* double bonds, ethers, sulfides, and oxime).[21–28] The practical applications of these probes are mostly limited by the delayed and monotonous response to ClO^-, tedious synthesis steps, low quantum efficiency, low water solubility, low biocompatibility, and subjection to interference by other active oxygen

Department of Chemistry, Shanxi Normal University, Linfen 041004, China.
E-mail: zhefengfan@126.com

† Electronic supplementary information (ESI) available. See DOI: 10.1039/d1nj00932j

‡ Xiaoye Wen and Li Yan contributed equally to this work.

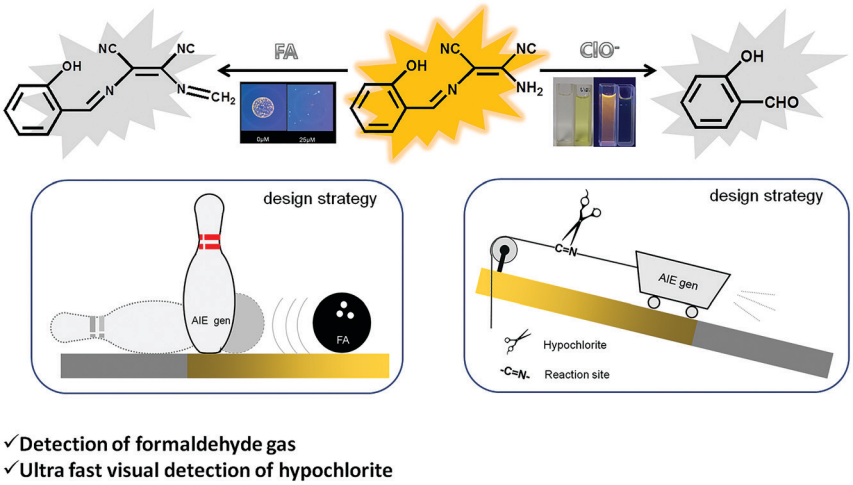

Scheme 1 Mechanism of the probe in detecting formaldehyde gas and hypochlorites.

substances.[29] Hence, new fluorescent probes are needed urgently to relieve the above limitations. Formaldehyde (FA, HCHO) is a colorless, combustible and suffocating chemical with high irritability, and is a ubiquitous toxin and carcinogen in the environment. Thus, residual FA in the environment and food can threaten human health.[30,31] The existing FA-responsive probes are mainly based on two reaction mechanisms:[32] (a) FA and methyl-allyl-amine undergo an aza-Cope rearrangement reaction to alter fluorescent signals;[33–36] (b) FA and the amino group ($-NH_2$) or hydrazine ($-NHNH_2$) undergo a condensation reaction to alter fluorescent signals.[37–39] Under physiological conditions, however, the probes based on the aza-Cope rearrangement reaction mostly respond very slowly to FA and usually take 2–3 h to reach the ideal fluorescent signals. In comparison, the fluorescent probes based on FA and hydrazine or amine reaction respond much faster.

Aggregation-induced emission (AIE) probes can solve the defects of aggregation concentration quenching in common luminescent materials, and are widely applied owing to the convenience of structural modification and fluorescence wavelength adjustment.[40–42] Our team has made many efforts to build structurally simple fluorescence sensors with high sensitivity, efficiency and practical values, and has constructed a series of AIE fluorescent probes from Schiff base derivatives. Moreover, through the modification of fluorescence molecular structures by introducing different groups, we have managed to adjust molecular energy gaps, forming fluorescent probes with emission at different wavelengths, and applied in the detection of single analytes or continuous detection of two analytes.[43–46] Recently, OR logic fluorescent probes have displayed many advantages and thus are increasingly needed and applied. In this regard, here we experimentally designed a novel simple double-site AIE fluorescent probe based on diaminomaleonitrile (DAMN). In brief, the convenient detection of hypochlorites and FA was realized by introducing different binding sites (C═N, $-NH_2$) in the structure of the probe. The response of the probe to ClO^- can be observed by the naked eye under sunlight as the solutions obviously changed in color so that the existence of ClO^- in the environment can be effectively detected in time. Moreover, the fluorescence spectral data can be used in further quantitative analysis of environmental ClO^-. Since AIE molecules show strong fluorescence under the solid-state, we prepared an FA gas-testing plate and thereby successfully detected gas-state FA. The one-step synthesis method used in this study is simple, cheap, biocompatible, and can be used in a 99% water medium. Hence, the new probe is prospective in practical applications and offers a new clue for constructing convenient double-site fluorescent probes (Scheme 1).

2. Experimental section

2.1. Materials and instruments

The reagents used in this experiment were purchased directly (Aladdin Co Ltd; China) and used without further purification. Ultrapure water with a resistivity of 18.2 MΩ cm was used in the experiment. The UV absorption spectrum was recorded on a UV-visible spectrophotometer (TU-1901; Purkinje General Instrument Co Ltd, China), the fluorescence spectrum was measured using a fluorospectrophotometer (LS55; PerkinElmer, USA). The NMR data were recorded on a magnetic resonance spectrometer (AVANCE III HD; Bruker), MS spectra were recorded on HRMS (Ultraflex MALDI-TOF/TOF, Bruker Daltonics, Germany). The surface morphology and particle size distribution were obtained using SEM (JSM-7500 F; Japan) and a particle size analyzer (Zetasizer Nano ZS90; Malvern Panalytical, UK), respectively. The infrared data were measured using an FT-IR Spectrometer (Varian-660-IR; USA). The buffer solution (Tris–HCl) was prepared using a pH meter (PHS-3E; China).

2.2. Synthesis steps

The one-step synthetic route of the probe is illustrated in Fig. 1. In brief, diaminomaleonitrile (DAMN) (5.0 mmol, 0.54 g) was

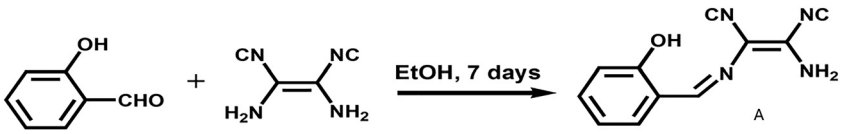

Fig. 1 Synthetic route of the probe.

dissolved in anhydrous ethanol (25 mL), and then salicylaldehyde (1.0 equiv.) was dripped dropwise. The reaction mixture was stirred at room temperature for 7 days, forming earthy yellow precipitates, which were washed in anhydrous ethanol and vacuum-dried. After that, the khaki target compound **A** (0.87 g) was obtained, with a yield rate of 82.04%. ^{1}H NMR (600 MHz, DMSO-d_6) δ (ppm) (Fig. S1a, ESI†): 10.42 (1H, s), 8.61 (1H, s), 8.05 (1H, dd, J7.8), 7.85 (2H, s), 7.41–7.30 (1H, m), 7.16–6.77 (2H, m). ^{13}C NMR (150 MHz, DMSO-d_6) δ (ppm) (Fig. S1b, ESI†): 158.61, 153.31, 133.67, 129.37, 126.51, 121.73, 119.89, 116.89, 114.73, 103.91. HRMS (ESI) (Fig. S2, ESI†): m/z calculated for $C_{11}H_8N_4O$: 212.07; found $[M + H]^+$: 213.08.

2.3. Common methods of spectral measurement

The compound was dissolved in dimethyl sulfoxide (DMSO) to form the reserve probe solution (1.0 mM). The concentration of other inorganic substances was 10 mM. The excitation wavelength for fluorescent spectrometry was 390 nm, and the excitation and emission slit widths were 5 and 20 nm, respectively. The fluorescence spectra and UV absorption spectra of the probe in DMSO–H_2O mixtures with different water fraction volumes (f_w = 0–99%) were recorded, and thereby the AIE properties of the probe were determined. The response of the probe to FA/ClO^- was monitored in DMSO/H_2O (1 : 99, v/v) at pH = 7.0 (Tris–HCl, 10 mM).

2.4. Preparation of portable solid-state sensor and analysis method of ClO^- in actual samples

The detection plate was a thin-layer chromatography (TLC) plate. The TLC plate was dripped with a DMSO/H_2O (1 : 99, v/v) probe solution (1 mM, pH = 7.0), and dried in a drying cabinet for 15 min. Then, the plate covered with the probe was observed in an ultraviolet analyzer (365 nm), where the yellow fluorescent zone was the detection area. Formaldehyde solutions at different concentrations were added in bottles, and the detection plate was rapidly hung in each bottle. The bottles were kept at 60 °C for 1 h, and after the FA gas was fully volatilized, the detection plates were taken out. The changes in fluorescent colors in the detection plates were observed under an ultraviolet lamp at 365 nm.

The probe was applied for ClO^- detection in real water samples, including drinking water (from a direct drinking system in a teaching building), lake water (from a lake in a campus), and tap water (from a laboratory). Lake water samples were filtered and diluted first. The actual water sample detection was performed by real-time sampling and real-time detection, which ensured the valid ClO^- concentrations in the water samples.

3. Results and discussion

3.1. Photophysical properties of the probe

The probe can be dissolved in common organic solvents, there was almost no emission in these solvents, but it showed a strong emission in 1% DMSO aqueous solution (Fig. 2a). The fluorescence emission spectra and UV absorption spectra of the probe in DMSO/H_2O mixtures were recorded, and thereby the AIE of the probe was determined. The emission spectra of the probe fell in the H_2O–DMSO system, and the fluorescence emission spectra of the solvent in different water fraction volumes (f_w) were recorded. Clearly, the probe showed very weak fluorescence emission in pure DMSO, and the fluorescence emission maximized in DMSO/H_2O (1 : 99, v/v) (Fig. 3a). UV absorption also proved the properties of AIE (Fig. 3b). In a good solvent DMSO, C–C of probe molecules can freely rotate, and the intramolecular rotation decreased the energy passing through non-radiative channels, so the probe has no fluorescence. In the

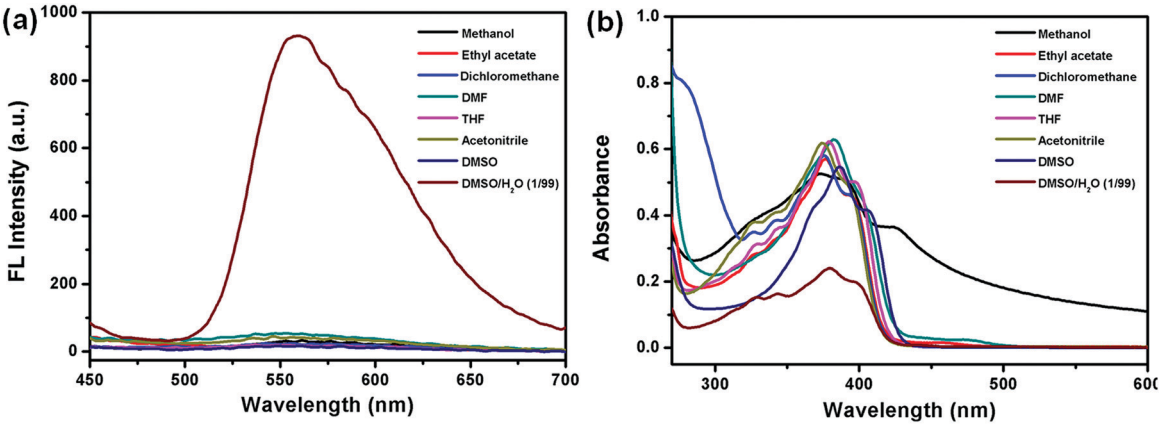

Fig. 2 (a) The fluorescence spectra and (b) the UV absorption spectrum of the probe in different organic solvents.

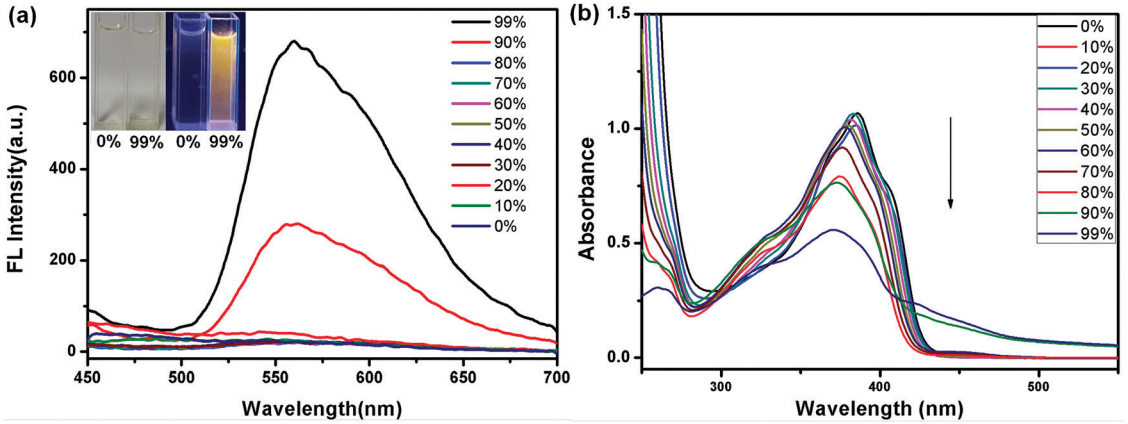

Fig. 3 (a) FL emission spectra of the probe; (b) UV absorption spectra of the probe in solvents with different water fraction volume (f_w).

solid- or aggregation-state (poor solvents), after the molecules were excited, the hydroxyl group and nitrogen atoms formed an intramolecular hydrogen bond, which initiated the excited-state intramolecular proton transfer, so the excited-state non-radiative energy decreased and the probability of radiative transition increased, causing AIE.[47–51] Quinine sulfate was used as a reference, based on $\Phi_x = \Phi_{st}(I_x/I_{st})(\eta_x^2/\eta_{st}^2)(A_{st}/A_x)$ (x, st are the tested substance and the reference, respectively; Φ, I, A, η are quantum yield, fluorescence integral area, absorbance, and solvent refractive index, respectively). The relative quantum yields of the probe in the pure DMSO solution and DMSO/H_2O (1 : 99, v/v) were calculated to be 3.47% and 40.67%, respectively. These results imply that the aggregation-state probe has high fluorescence quantum yield and can effectively

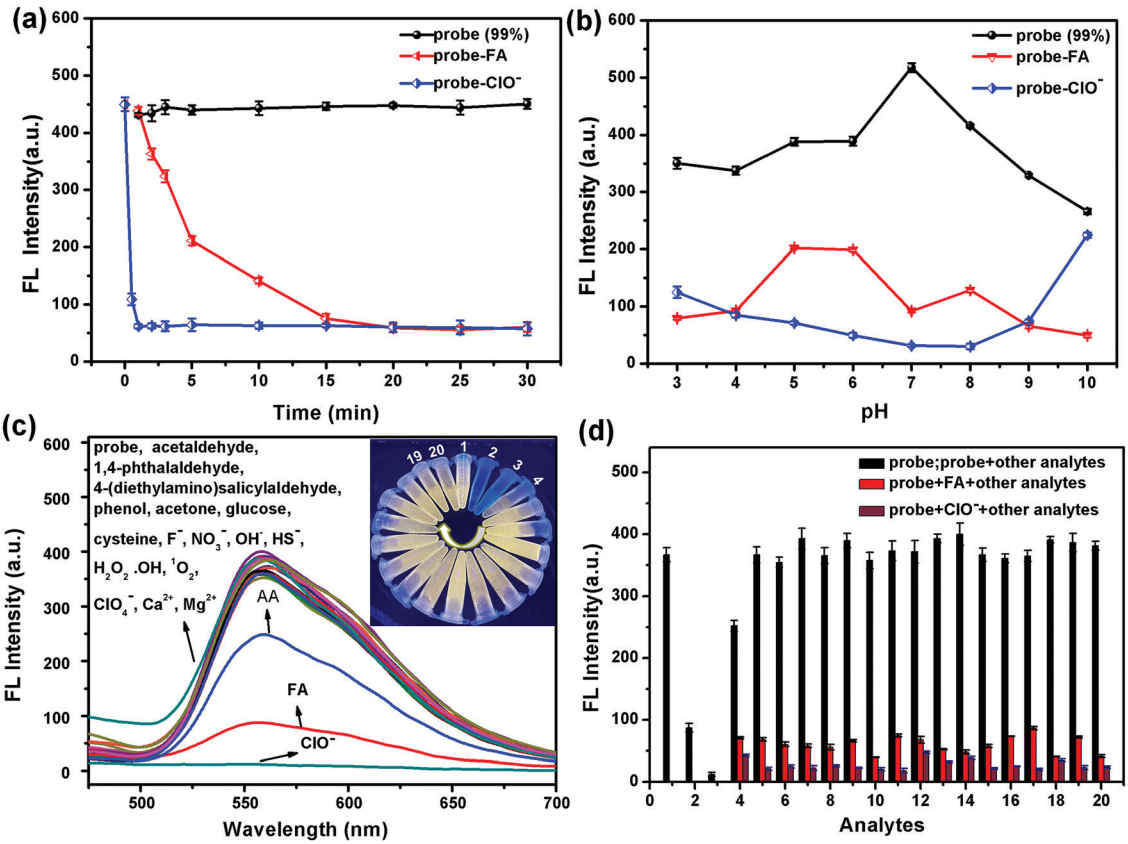

Fig. 4 (a) Fluorescence intensity changes of the probe in response to ClO^- and FA within 30 min; (b) effects of pH on fluorescence intensity of the probe response to ClO^- and FA; (c) fluorescence spectra of the probe after the addition of 5 equiv. of different competitive substances; (d) fluorescence of the probe when the tested substances and 5 equiv. of other competitive substances coexisted (1. probe, 2. formaldehyde, 3. ClO^-, 4. acetaldehyde, 5. 1,4-phthalaldehyde, 6. 4-(diethylamino) salicylaldehyde, 7. phenol, 8. acetone, 9. glucose, 10. cysteine, 11. F^-, 12. NO_3^-, 13. OH^-, 14. HS^-, 15. H_2O_2, 16. $^{\bullet}OH$, 17. $^1O_2$, 18. ClO_4^-, 19. Ca^{2+}, 20. Mg^{2+}).

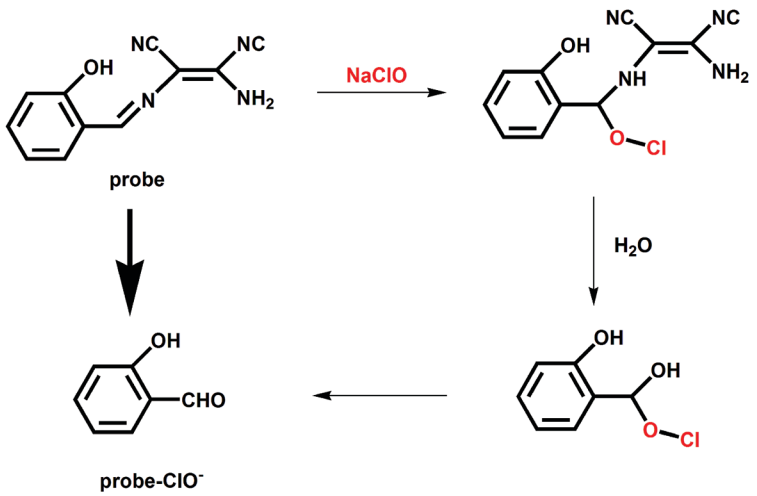

Scheme 2 Reaction mechanism between the probe and ClO^-.

improve precision and sensitivity. The dispersed particle sizes of the probe in different solvents were detected using dynamic light scattering (DLS, Fig. S3, ESI†). In DMSO/H_2O (1 : 99, v/v), the dispersed particle size of the probe was significantly enlarged.

3.2. Mechanism of the probe in double-site detection of FA and ClO^-

The reaction time is a critical factor that reflects the feasibility and practicability of a probe. Firstly, changes in responsive light intensity of the new probe with ClO^- and FA within 30 min were detected. The fluorescence intensity of the probe did not change with time (Fig. 4a). After the addition of ClO^-, the fluorescence intensity of the probe was weakened immediately, and fluorescence was quenched within the 30 s and minimized within 1 min, indicating the probe rapidly responds to ClO^- and is very important for real-time detection of ClO^-. The response time of the probe over FA was studied, which showed the quenching effect of the probe was optimized after 20 min. Thus, the optimal FA detection time of the probe was set at 20 min. Moreover, to validate the practicability of the probe over real samples, we explored the effect of pH on the probe (Fig. 4b). Though acidity is favorable for the rapid formation of Schiff base compounds, the stability of Schiff bases is also affected.[52] The deprotonation under base conditions can improve the solubility of the probe and weaken its aggregation and fluorescence. After careful consideration, the detection condition of the probe over formaldehyde and ClO^- was set at pH = 7.0 in subsequent fluorescence detection. The optical response of the probe over other analytes was also studied (Fig. 4c). Some potentially competitive micromolecular substances or ions (aldehyde, 1,4-phthalaldehyde, 4-(diethylamino)salicylaldehyde, phenol, acetone, glucose, cysteine, F^-, NO_3^-, OH^-, HS^-, H_2O_2, $^{\bullet}OH$, $^1O_2$, ClO_4^-, Ca^{2+}, and Mg^{2+}) were added to detect the variations of fluorescence emission signals and the specificity of the probe. The weak fluorescence changes of all substances can be ignored, except acetaldehyde. Though other aldehydes can also interact with the probe to form Schiff base compounds, such reactions are usually very slow and take hours, so that these substances do not interfere with formaldehyde detection within the tested 20 min. The effects of other coexisting competitive substances were studied during the detection of FA and ClO^- (Fig. 4d). Results showed that the specific detection of the probe was unaffected by other potentially competitive small molecules, active oxygen species, or ions. Though the response of the probe to FA and ClO^- implied the quenching of fluorescent signals, the presence of FA did not largely affect the timely detection of ClO^-, since the response time and temperature both largely differed between FA and ClO^-. Thus, FA and ClO^- can be effectively differentiated by the response time-duration of the probe.

3.3. Fluorescence-sensing performance on ClO^-

In Scheme 2, the sensing mechanism of the probe over NaClO is proposed, in which C═N is an effective recognition site of ClO^-, and ClO^- can induce the conversion from C═N to –CHO. When the probe molecules were under the aggregation state, the existence of intramolecular hydrogen bond led to an excited-state intramolecular proton transfer (ESIPT), but after the addition of ClO^-, the intramolecular hydrogen bond was destroyed and ESIPT was interrupted, leading to quenching of fluorescence. The recognition mechanism of the probe was validated by high-resolution mass spectrometry (Fig. S4, ESI†). When the probe

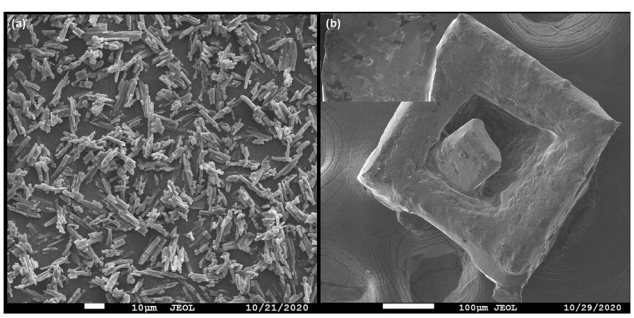

Fig. 5 SEM images before and after the reaction between the probe and ClO^-.

molecules reacted with 1 equiv. of NaClO, the products were recrystallized. The mass spectrometry peaks at *m*/*z* 163.157 corresponded to the oxidation products $[C_7H_6O_2 + H_2O + Na]^+$, indicating that the probe effectively bound to ClO^-. Moreover, the infrared spectra and scanning electron microscopy (SEM) images were both compared before and after the binding between the probe and ClO^-, which further uncovered the binding between the probe and ClO^-. Several assignment peaks with obvious variations were found

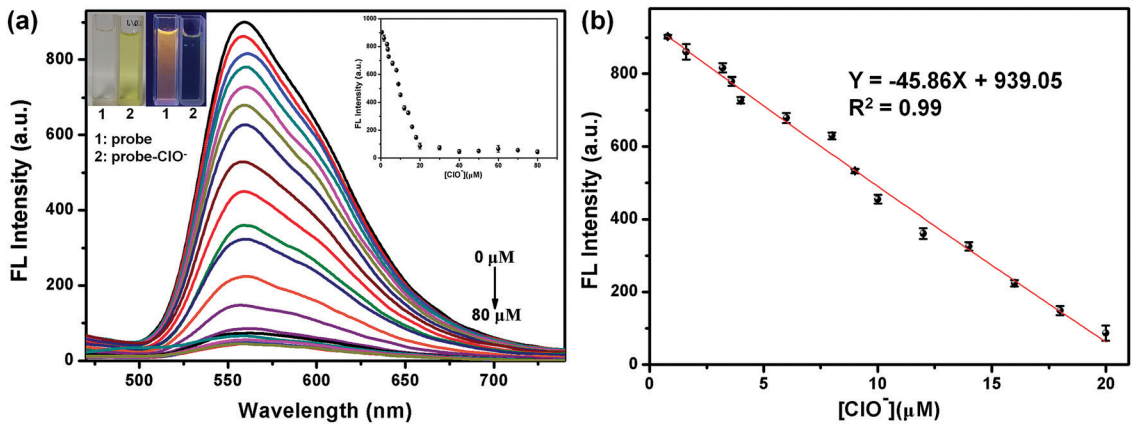

Fig. 6 (a) Fluorescence spectra of the probe (20 μM) added with different concentrations of ClO^- (0–80 μM); inset: pictures of the probe/probe-ClO^- under daylight lamp or 365 nm UV lamp; (b) working curves of the probe and ClO^- at different concentrations.

Table 1 Comparison of different ClO^- detection probes

Probe	One-step synthesis	Medium (v/v)	Fluorescent color	Fluorescent behavior	Linear range (μM)	LOD (μM)	Ref.
CDs	NO	PBS	Blue	On–off	0.0–36.0	0.47	53
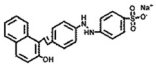	NO	DMSO/PBS (2/8)	Orange	Off–on	0–500	0.058	21
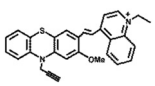	YES	PBS	Green	On–off	0–20	0.0082	54
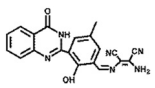	NO	PBS/DMSO (2/1)	Blue	Off–on	0–20	0.012	20
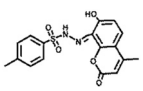	NO	PBS/DMSO (99/1)	Blue	Off–on	0–15	0.0091	29
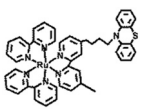	NO	PBS	Blue	Off–on	0–100	0.018	55
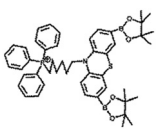	NO	DMSO/H_2O (1/99)	Blue	Ratiometric	0–10	0.41	56
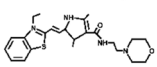	No	H_2O	Green	On–off	10–32	0.17	57
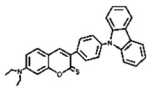	No	ACN/H_2O (1/1)	Blue	Off–on	—	0.17	58
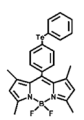	No	PBS/CH_3CN (7/3)	Green	Off–on	0–8	0.12	59
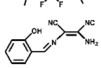	YES	DMSO/H_2O (1/99)	Yellow	On–off	0.70–20	0.018	This work

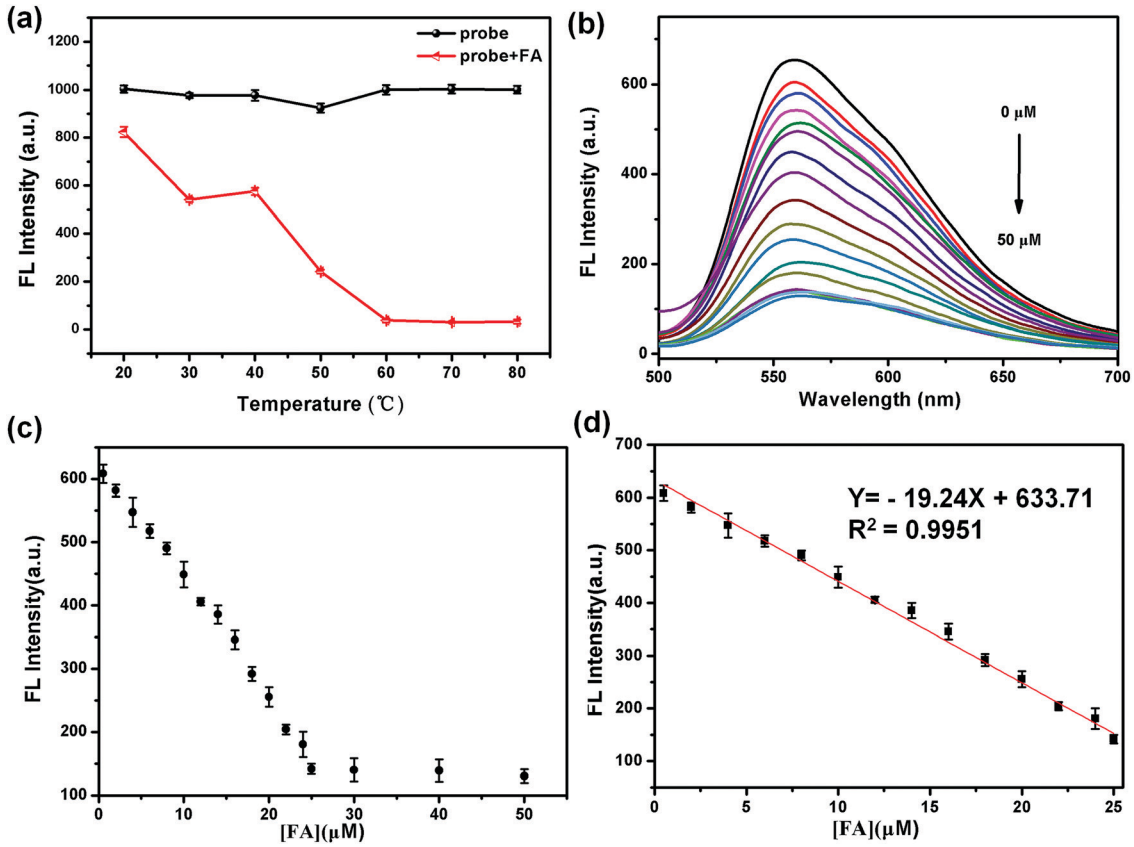

Fig. 7 (a) Effects of temperature on the fluorescence intensity of the probe in response to FA; (b) fluorescence spectra of the probe (25 μM) added with FA (0–50 μM); (c) Scatter plot of the probe and FA at different concentrations (0–50 μM); (d) working curve of the probe and FA at different concentrations (0–25 μM).

in FT-IR spectra (Fig. S5, ESI†). When the probe bonded with ClO^-, the peak of the exposed amino group ($-NH_2$) at 3345–3459 cm^{-1} was largely weakened, the assignment peak of cyano (C≡N) at 2239 cm^{-1} disappeared, and a new assignment peak appeared at 1798 cm^{-1} (C=O), suggesting ClO^- reacted with the probe. SEM more visually reflected the changes in the probe after binding with ClO^- (Fig. 5). Clearly, the probe is a clustered short rod and reacts with ClO^- to form a decentralized massive structure, indicating that the structure changed-significantly after the reaction. Furthermore, the different morphology structure of the probe corresponds to the fluorescence change of the probe before and after the reaction with ClO^-. The morphology of the probe changes from the aggregate state to the dispersed state accompanied by quenching of the strong fluorescence based on AIE and ESIPT. All the studied results confirmed the mechanism of detection on ClO^-.

After ClO^- was added to the probe solution, the colorless and transparent solution immediately turned yellow under sunlight, which corresponds to the fluorescence quenching of the probe under the UV lamp at 365 nm. The color changes after the reaction between the probe and ClO^- indicate that the probe can recognize ClO^- under the naked eye. After ClO^- at different concentrations was added to the probe DMSO/H_2O solution (1 : 99, v/v), the responsive sensitivity of the probe to ClO^- was evaluated. Under the optimal experimental conditions (Fig. 6), as the ClO^- concentration increased, fluorescence was gradually lowered, and the probe responded to ClO^- within 0.70–20 μM in a linear way, with the correlation coefficient of 0.99. The detection limit of the probe was determined by $3\delta/k$ to be 18 nM (δ is standard deviation, k is the slope of the standard curve equation). All results indicated that the probe can rapidly and visually detect ClO^-, and has high selectivity and sensitivity as well as broad application prospects.

To evaluate the feasibility and novelty of the ClO^- responsive probe, we compared it with other ClO^- fluorescent probes (Table 1). The new probe shows multiple excellent analytical characteristics, such as simple synthesis steps, long emission wavelength, and use of a highly aqueous medium.

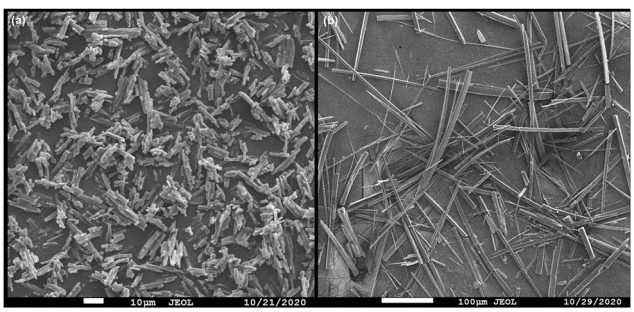

Fig. 8 SEM images before and after the reaction between the probe and FA.

3.4. Fluorescence sensing performance of the probe over FA

The effects of temperature on the probe and its response to FA solutions were investigated (Fig. 7a). Results show that the probe has high stability, and its fluorescence intensity is not largely affected by temperature, but the temperature above 60 °C is favorable for its binding with FA, which may be because aldehyde amine is condensed to form Schiff bases. The experimental conditions of the probe for FA detection were set at 20 min, 60 °C, pH = 7.0. Then, the fluorescence spectra of the probe in FA solutions at different concentrations were observed. The fluorescence quenching effects of FA at different concentrations on the probe were compared. Results show that the fluorescence

Table 2 Comparison of different FA detection probes

Probe	One-step synthesis	Medium (v/v)	Emission wavelength (nm)	Analytes	LOD (μM)	Gas test paper	Ref.
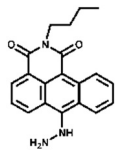	No	MeOH	600	FA	0.12	Yes	60
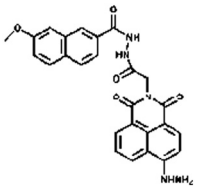	No	DMSO/PBS 1 : 99	550	FA	0.0058	No	61
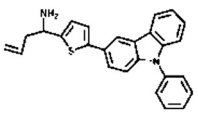	No	H_2O/DMSO 3 : 7	393	FA	1.6	Yes	62
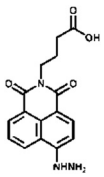	No	DMSO/PBS 1 : 1	519	FA	0.36	No	63
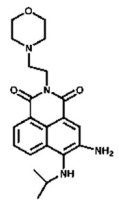	No	PBS	444	FA	0.27	No	64
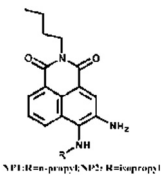	No	PBS/EtOH 5 : 95	450	FA	1.6, 1.8	No	65
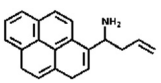	Yes	EtOH/HEPES 1 : 99	472	FA	0.11	No	34
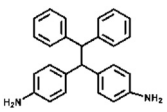	No	DMSO/PBS 1 : 9	530	FA	0.040	No	38
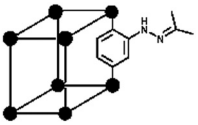	No	H_2O	436	FA	8.4	No	66
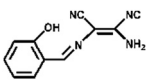	Yes	H_2O/DMSO 1 : 99	575	FA	0.042	Yes	This work

Table 3 Detection of ClO^- in real samples by the probe

	Sensor (μM)	Added (μM)	Found (μM)	Recovery (%)
Purified water	No detected	5.0	5.74 ± 0.55	114.8
		10.0	9.68 ± 0.24	96.8
Tap water	4.89 ± 0.11	5.0	10.36 ± 0.67	109.4
		10.0	15.04 ± 0.34	101.5
Lake water	No detected	5.0	5.16 ± 0.06	103.2
		10.0	11.05 ± 0.03	110.5

intensity of the probe is well linearly related to the FA concentration within 0.50–25 μM (Fig. 7b–d). Calculations indicate that the detection limit of FA was 42 nM. The above results suggest that the new probe can quantitatively detect aqueous FA and has high sensitivity. The high fluorescence-sensing ability of the probe over FA may be attributed to the intramolecular charge transfer of the excited probe, forming an electron push/pull system. Since the probe has a strong fluorescence, when the exposed amino group binds with FA, the push–pull electron system is destroyed, so fluorescence is quenched. The probe and FA-binding mode were explored through fluorescence spectral analysis. This was validated by mass spectra (Fig. S6, ESI†). The MS peak of the product $[C_{12}H_8N_4O + H_2O + H]^+$ from the reaction between the probe and 1 equiv. of FA appeared at *m/z* 243.14, indicating that the probe can effectively bind with FA. SEM also shows that after binding with formaldehyde, the probe changed from the original clustered short rod shape to a decentralized fine and long fiber-like structure, which corresponds to the fluorescence change of the probe before and after the reaction with FA (Fig. 8). The product was further purified and characterized by FT-IR (Fig. S7, ESI†), the bimodal absorption between 3345–3459 cm^{-1} was assigned to $-NH_2$. When the probe bonded with FA, the disappearance of the bimodal absorption corresponding to the disappearance of $-NH_2$, the appearance of spikes (1516 cm^{-1}) indicated the formation of new imine groups. All the studied results confirmed the mechanism of the detection on FA.

To evaluate the feasibility of the new FA-responsive probe, we compared it with other FA fluorescent probes (Table 2). The new probe shows multiple excellent analytical characteristics, such as the one-step synthesis, emission at long wavelengths, and applicability to gas detection.

3.5. Practical application of the probe

The probe was used to detect ClO^- in real samples collected from water environments, including lake water, tap water, and drinking water. Each experiment was conducted in triplicate to ensure experimental accuracy and validity (Table 3). From the standard curves of the probe in response to ClO^-, we determined acceptable recovery rates, indicating that the probe is feasible in detecting ClO^- in real environments.

To further validate the detection ability of the probe over FA gas, we developed an FA gas detection plate (Fig. 9). Under ultraviolet illumination at 365 nm, as the FA gas concentration was increased, the fluorescence of the probe gradually weakened and finally disappeared. Hence, the experimental results indicate that the probe can be used as a portable fluorescence sensor for detecting gas-phase FA. This method is operationally easy and cheap and offers a feasible clue for the FA gas detection.

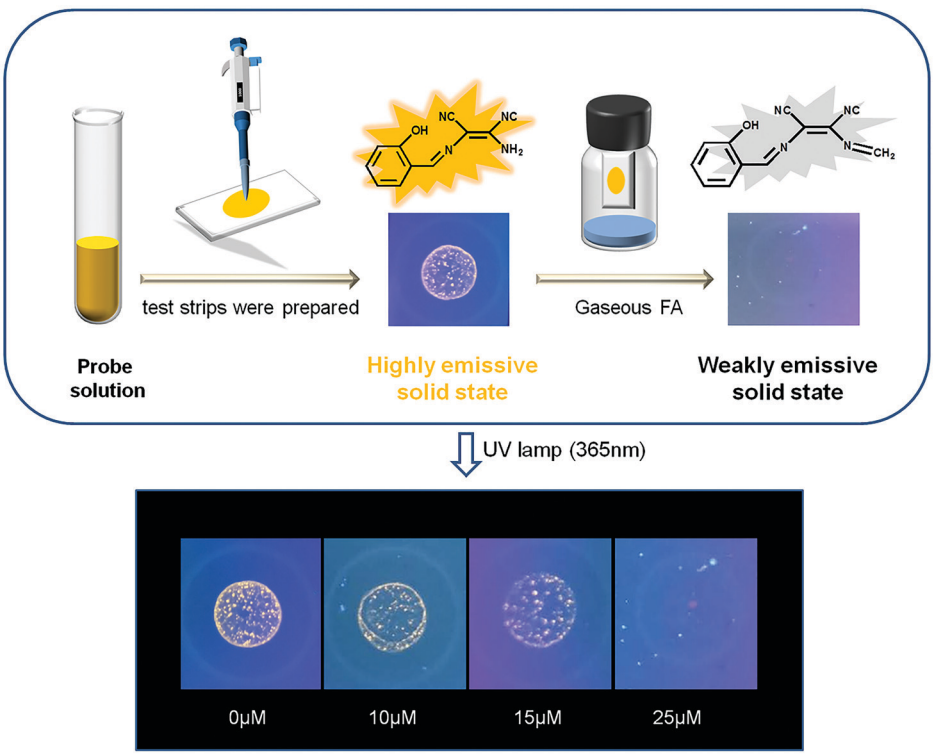

Fig. 9 Fluorescence pictures of gas-state FA on the detection plate (UV lamp at 365 nm).

4. Conclusion

An aggregation-induced emission (AIE) probe based on diaminomaleonitrile was fabricated and used to sensitively and efficiently detect FA and hypochlorites. This probe can be synthesized easily from cheap raw materials and has typical AIE. In the mixed solvent of DMSO/H_2O (1 : 99, v/v), the detection of ClO^- by the probe was fast, visible to the naked eye, and sensitive. The detection limit was as low as 18 nM, and the recovery of real water samples also validated the probe's practicability for ClO^- detection. Based on the condensation reaction, the probe with an amino group as the binding site can well linearly detected in 0.50–25 μM FA solutions, with the detection limit of 42 nM. According to AIE molecules' application in solid films, a type of portable solid-state detection plate was successfully developed and used to detect FA gas.

In short, the simply synthesized probe is multifunctional. It breaks through the defects of other probes such as complex synthesis steps and organic solvent dependence. It is a novel probe and can realize the detection of samples in the environmental field. The probe has a good application prospect for the rapid visual detection of ClO^- in environmental water sample detection. The construction of solid-state detection plates has favorable application prospects and provides a new idea for the monitoring of formaldehyde gas in the environment. The establishment and research on the new method offer a new technique and clues for double-site fluorescence detection of gas-state FA and hypochlorites.

Author contributions

Xiaoye Wen and Li Yan contributed equally to this work: conceptualization, data curation, formal analysis, methodology, investigation, writing-original draft. Zhefeng Fan: investigation, resources, supervision, writing-review & editing.

Conflicts of interest

There are no conflicts of interest to declare.

Acknowledgements

This work was supported by the Doctor Fund of Shanxi Normal University (0505/02070481), Science Foundation for Youths Fund of Shanxi Province of China (0502/02010163).

References

1 Y. Wu, J. Wang, F. Zeng, S. Huang, J. Huang, H. Xie, C. Yu and S. Wu, *ACS Appl. Mater. Interfaces*, 2016, **8**, 1511–1519.
2 M. Vendrell, D. Zhai, J. C. Er and Y. T. Chang, *Chem. Rev.*, 2012, **112**, 4391–4420.
3 B. Dong, X. Song, C. Wang, X. Kong, Y. Tang and W. Lin, *Anal. Chem.*, 2016, **88**, 4085–4091.
4 Y. Chen, *Anal. Biochem.*, 2020, **612**, 113900.
5 S. Mu, H. Gao, C. Li, S. Li, Y. Wang, Y. Zhang, C. Ma, H. Zhang and X. Liu, *Talanta*, 2021, **221**, 121606.
6 G. Li, Y. Ma, M. Pei and W. Lin, *Anal. Chem.*, 2019, **91**, 14586–14590.
7 H. Ren, F. Huo, Y. Zhang, S. Zhao and C. Yin, *Sens. Actuators, B*, 2020, **319**, 128248.
8 C.-G. Dai, X.-L. Liu, X.-J. Du, Y. Zhang and Q.-H. Song, *ACS Sens.*, 2016, **1**, 888–895.
9 Y.-L. Qi, L.-L. Chen, L. Guo, Y.-Y. Cao, H.-R. Wang, Y.-S. Yang, Y.-D. Lu and H.-L. Zhu, *Appl. Mater. Today*, 2020, **21**, 100877.
10 P. Q. Nhien, W. L. Chou, T. T. K. Cuc, T. M. Khang, C. H. Wu, N. Thirumalaivasan, B. T. B. Hue, J. I. Wu, S. P. Wu and H. C. Lin, *ACS Appl. Mater. Interfaces*, 2020, **12**, 10959–10972.
11 X. Wen, Q. Wang and Z. Fan, *Anal. Chim. Acta*, 2018, **1013**, 79–86.
12 Z. Zhou, X. Li, Y. Zhang, C. C. Zhang, Y. Tang, J. Gao, L. Ma and Q. Wang, *Mater. Sci. Eng., C*, 2019, **99**, 1092–1098.
13 X. Wen, L. Yan and Z. Fan, *J. Photochem. Photobiol., A*, 2021, **405**, 112969.
14 Z. H. Xu, Y. Wang, Y. Wang, J. Y. Li, W. F. Luo, W. N. Wu and Y. C. Fan, *Spectrochim. Acta, Part A*, 2019, **212**, 146–154.
15 M. Pannipara, A. G. Al-Sehemi, A. Irfan, M. Assiri, A. Kalam and Y. S. Al-Ammari, *Spectrochim. Acta, Part A*, 2018, **201**, 54–60.
16 X. Li, X. Lin, S. Lin, X. Sun, D. Gao, B. Liu, H. Zhao, J. Zhang, S. Cong and L. Wang, *ACS Appl. Nano Mater.*, 2019, **2**, 3161–3168.
17 Y. Zhan, F. Luo, L. Guo, B. Qiu, Y. Lin, J. Li, G. Chen and Z. Lin, *ACS Sens.*, 2017, **2**, 1684–1691.
18 C. Ye, H. Yuan, Z. Lou and N. Zhu, *Energy Fuels*, 2016, **30**, 2990–2996.
19 M. Li, F. Du, P. Xue, X. Tan, S. Liu, Y. Zhou, J. Chen and L. Bai, *Spectrochim. Acta, Part A*, 2020, **227**, 117760.
20 Y. Li, L. Liu, Y. Tang, Y. Wang, J. Han and L. Ni, *Spectrochim. Acta, Part A*, 2020, **232**, 118154.
21 B. Zhu, X. Wu, J. Rodrigues, X. Hu, R. Sheng and G. M. Bao, *Spectrochim. Acta, Part A*, 2021, **246**, 118953.
22 J. Shepherd, S. A. Hilderbrand, P. Waterman, J. W. Heinecke, R. Weissleder and P. Libby, *Chem. Biol.*, 2007, **14**, 1221–1231.
23 X. Cheng, H. Jia, T. Long, J. Feng, J. Qin and Z. Li, *Chem. Commun.*, 2011, **47**, 11978–11980.
24 Q. Hu, C. Qin, L. Huang, H. Wang, Q. Liu and L. Zeng, *Dyes Pigm.*, 2018, **149**, 253–260.
25 Y. Koide, Y. Urano, K. Hanaoka, T. Terai and T. Nagano, *J. Am. Chem. Soc.*, 2011, **133**, 5680–5682.
26 Y. Huang, Y. Zhang, F. Huo, J. Chao and C. Yin, *Sens. Actuators, B*, 2019, **287**, 453–458.
27 Y. Huang, Y. Zhang, F. Huo, Y. Liu and C. Yin, *Dyes Pigm.*, 2020, **179**, 108387.
28 Y. Shi, F. Huo, Y. Zhang and C. Yin, *The Analyst*, 2020, **145**, 7297–7302.
29 Y. Tang, Y. Li, L. Liu, H. Ni, J. Han, L. Wang, Y. Mao, L. Ni and Y. Wang, *J. Photochem. Photobiol., A*, 2020, **387**, 112166.
30 H.-W. Chen, H. Li and Q.-H. Song, *ACS Omega*, 2018, **3**, 18189–18195.
31 T. F. Brewer and C. J. Chang, *J. Am. Chem. Soc.*, 2015, **137**, 10886–10889.

32 X. Liu, N. Li, M. Li, H. Chen, N. Zhang, Y. Wang and K. Zheng, *Coord. Chem. Rev.*, 2020, **404**, 213109.
33 B. Zhai, Y. Zhang, Z. Hu, J. He, J. Liu, C. Gao and W. Li, *Dyes Pigm.*, 2019, **171**, 107743.
34 D. Zhang, D. Liu, M. Li, Y. Yang, Y. Wang, H. Yin, J. Liu, B. Jia and X. Wu, *Anal. Chim. Acta*, 2018, **1033**, 180–184.
35 T. Gao, X. Cao, A. Bi, J. Dong, S. Huang, X. Huang, S. Wen and W. Zeng, *Sens. Actuators, B*, 2018, **273**, 1139–1145.
36 Y. Zhou, J. Yan, N. Zhang, D. Li, S. Xiao and K. Zheng, *Sens. Actuators, B*, 2018, **258**, 156–162.
37 K. Wechakorn, S. Supalang and S. Suanpai, *Tetrahedron*, 2020, **76**, 131411.
38 W. Chen, J. Han, X. Wang, X. Liu, F. Liu, F. Wang, R. Q. Yu and J. H. Jiang, *ACS Omega*, 2018, **3**, 14417–14422.
39 A. Bi, T. Gao, X. Cao, J. Dong, M. Liu, N. Ding, W. Liao and W. Zeng, *Sens. Actuators, B*, 2018, **255**, 3292–3297.
40 M. Gao and B. Z. Tang, *ACS Sens.*, 2017, **2**, 1382–1399.
41 Z. He, C. Ke and B. Z. Tang, *ACS Omega*, 2018, **3**, 3267–3277.
42 X. Li, K. Ma, S. Zhu, S. Yao, Z. Liu, B. Xu, B. Yang and W. Tian, *Anal. Chem.*, 2014, **86**, 298–303.
43 X. Wen and Z. Fan, *Sens. Actuators, B*, 2017, **247**, 655–663.
44 X. Wen and Z. Fan, *Anal. Chim. Acta*, 2016, **945**, 75–84.
45 Q. Wang, X. Wen and Z. Fan, *J. Photochem. Photobiol., A*, 2018, **358**, 92–99.
46 L. Yan, X. Wen and Z. Fan, *Anal. Bioanal. Chem.*, 2020, **412**, 1453–1463.
47 V. S. Padalkar and S. Seki, *Chem. Soc. Rev.*, 2016, **45**, 169–202.
48 B. K. Paul and N. Guchhait, *J. Lumin.*, 2012, **132**, 2194–2208.
49 A. C. Sedgwick, L. Wu, H. H. Han, S. D. Bull, X. P. He, T. D. James, J. L. Sessler, B. Z. Tang, H. Tian and J. Yoon, *Chem. Soc. Rev.*, 2018, **47**, 8842–8880.
50 A. J. Stasyuk, P. J. Cywiński and D. T. Gryko, *J. Photochem. Photobiol., C*, 2016, **28**, 116–137.
51 Z. Zhang, Y.-A. Chen, W.-Y. Hung, W.-F. Tang, Y.-H. Hsu, C.-L. Chen, F.-Y. Meng and P.-T. Chou, *Chem. Mater.*, 2016, **28**, 8815–8824.
52 C. Dohno, A. Okamoto and I. Saito, *J. Am. Chem. Soc.*, 2005, **127**, 16681–16684.
53 C. J. Rha, H. Lee and C. Kim, *Inorg. Chem. Commun.*, 2020, **121**, 108244.
54 J. Guo, S. Ye, H. Li, J. Song and J. Qu, *Spectrochim. Acta, Part A*, 2020, **240**, 118592.
55 F. Liu, Y. Gao, J. Wang and S. Sun, *The Analyst*, 2014, **139**, 3324–3329.
56 L. Wang, Y. Hu, Y. Qu, J. Xu and J. Cao, *Dyes Pigm.*, 2016, **128**, 54–59.
57 L. L. Gao, W. W. Wang, W. N. Wu, Y. Wang, X. L. Zhao, Y. C. Fan, H. J. Li and Z. H. Xu, *Spectrochim. Acta, Part A*, 2020, **231**, 118110.
58 V.-N. Nguyen, S. Heo, S. Kim, K. M. K. Swamy, J. Ha, S. Park and J. Yoon, *Sens. Actuators, B*, 2020, **317**, 128213.
59 W.-J. Shi, Y. Huang, W. Liu, D. Xu, S.-T. Chen, F. Liu, J. Hu, L. Zheng and K. Chen, *Dyes Pigm.*, 2019, **170**, 107566.
60 J. Chen, K. Chen, B. Han, Y. Xue, W. Chen, Z. Gao and X. Hou, *Tetrahedron*, 2020, **76**, 131681.
61 G. Yuan, H. Ding, L. Peng, L. Zhou and Q. Lin, *Food Chem.*, 2020, **331**, 127221.
62 J. Gu, X. Li, G. Zhou, W. Liu, J. Gao and Q. Wang, *J. Hazard. Mater.*, 2020, **386**, 121883.
63 W. Yuan, X. zhong, Q. Han, Y. Jiang, J. Shen and B. Wang, *J. Photochem. Photobiol., A*, 2020, **400**, 112701.
64 S. Cai, C. Liu, J. Gong, S. He, L. Zhao and X. Zeng, *Spectrochim. Acta, Part A*, 2021, **245**, 118949.
65 S. Cai, C. Liu, X. Jiao, L. Zhao and X. Zeng, *Tetrahedron*, 2020, **76**, 131617.
66 S. Nandi, E. Sharma, V. Trivedi and S. Biswas, *Inorg. Chem.*, 2018, **57**, 15149–15157.